Composites Part B 111 (2017) 228–234

Contents lists available at ScienceDirect

Composites Part B

journal homepage: www.elsevier.com/locate/compositesb

Investigation for surface finish improvement of FDM parts by vapor smoothing process

Rupinder Singh [a,*], Sunpreet Singh [a], Iqwinder Preet Singh [a], Francesco Fabbrocino [b], Fernando Fraternali [c]

[a] *Production Engineering Department, GNDEC, Ludhiana, 141006, India*
[b] *Department of Engineering, Pegaso University, Piazza Trieste e Trento, 48, Naples, 80132, Italy*
[c] *Department of Civil Engineering, University of Salerno, Via Giovanni Paolo II, 132, Fisciano, SA, 84084, Italy*

ARTICLE INFO

Article history:
Received 31 October 2016
Accepted 30 November 2016
Available online 30 November 2016

Keywords:
Fused deposition modelling
Surface finish
Dimensional accuracy
Vapor smoothing
Acetone
Design of experiment

ABSTRACT

Fused deposition modelling (FDM) is one of the most widely used cost-effective additive manufacturing (AM) technique for modelling and prototyping of functional/non-functional parts subjected to different industrial applications. However, this technique still possesses substantial problems in-terms of poor surface finish and dimensional accuracy of the prototypes. In the present research work, an effort has been made to improve the surface finish of FDM based benchmarks through chemical (acetone) exposure by using vapor smoothing station (VSS). Experimental analysis has been carried out by using design of experiments (DOE) technique in-order to find out the effect of input factors on surface finish of the benchmarks. The results of the present study highlights the capability of the VSS for improving the surface finish of the FDM based parts to nano-level with negligible dimensional deviations.

1. Introduction

There are number of "*Additive Manufacturing*" (AM) techniques that are used for fabricating 3-D solid models using virtual data by eliminating geometric restrictions [1]. These technologies are no longer expensive and their users are increasing day-by-day. The applications of AM technologies are not limited as industries are willing to use them at different stages such as: conceptual design, market evaluation, final verification and manufacturing analysis [2]. In recent past, AM technologies have progressed as a fabrication method for rapid tooling/finished products in low and medium batch production runs [3]. With the invention of two-axis high-speed motion control systems the building speed in significantly improved by 500% [4].

Fused deposition modelling (FDM) is one of the most widely used AM techniques which is being used to assist various production processes [5]. FDM system fabricates parts, layer-by-layer, by depositing semi-molten thermoplastic material in the form of thin slices on a fixtureless platform [6]. In the basic mechanism of FDM, a virtual model is converted into. STL (Standard Triangulation Language) format and opportunely oriented [7]. The deposition of the thermoplastic is carried out by the extrusion through a temperature controlled extrusion head. The chamber of the system is maintained at constant temperature (72 °C in case of acrylonitrile-butadiene-styrene) above the glass transition temperature in order to relax the thermal stresses and to solidify the deposited material. The base material is also used along with the model material which supports the overhanging geometries. After the completion of the part the traces of the base material is removed from the part manually (in case of simple geometries) or chemically (for deep cavities). FDM system offers numerous benefits like: ease of implementation, minimum product material, ease of support removal, ability to fabricate functional part, etc make this technique suitable for numerous applications in aerospace, automotive, biomedical and tooling [8,9]. The various applications of FDM parts are illustrated in Fig. 1.

The use of FDM parts in different applications is still questionable as the final part suffers from rough geometrical textures (due to staircase effect) and less geometrical tolerances in comparison of other AM technologies. However, various researchers have preformed several experimental/theoretical investigations to evaluate/predict the surface roughness and dimensional features of FDM parts [10–13]. It has been found that the layer thickness and part

* Corresponding author.
E-mail addresses: rupindersingh78@yahoo.com (R. Singh), prod@gndec.ac.in (S. Singh), prod@gndec.ac.in (I.P. Singh), francesco.fabbrocino@unipegaso.it (F. Fabbrocino), f.fraternali@unisa.it (F. Fraternali).

http://dx.doi.org/10.1016/j.compositesb.2016.11.062
1359-8368/

orientation affect the surface finish of the FDM parts [14]. According to a reported literature, it has been found that layer thickness is most influencing process parameter for the surface finish in comparison of road width and deposition speed [15]. In an another research work, a model was proposed for analyzing the affect of cross-sectional shape, surface angle, layer thickness and overlap between adjacent layers on surface quality [16]. Empirical values of surface roughness having non-uniform distribution of roughness over partial regions of the test model can be used to present actual surface roughness [17]. Hot cutter machining was found as a useful method for improving the surface finish of the FDM parts [13], however the improvements were not up to the marks as required for biomedical applications.

FDM parts were found to have dimensional variations at different geometrical section. It has been found that the shrinkage was dominant along length and width direction of built part whereas positive deviation (from the required value) was observed in the thickness direction [18].

New techniques, for testing dimensional accuracy and surface finish of prototypes, were developed by various researchers [19]. The optimum orientation was used through the application of genetic algorithm in order to enhance the surface finish with reduced build time [20]. Apart from the significant research efforts made by various researchers, knowledge of the optimum prototyping parameters of FDM system is still vital. A group of researchers have investigated the dimensional accuracy of FDM parts (having six features) and found part size, location in the work envelope and envelope temperature as significant parameters for dimensional accuracy [21]. One other group has used dimethyl-ketone-water based solution for improving the surface finish of FDM parts. The results of the study indicated significant improvements in the surface finishing [13]. According of literature review, the basic method/approaches for improving the surface finish (without affecting dimensional features) can by: by parametric optimization, empirical and analytical modelling, micro machining of FDM parts, coating & painting and chemical treatment.

Recently, Stratasys Inc. has introduced vapor smoothing station (VSS) for improving the surface finishing of the FDM parts. This system works on a standard procedure recommended by the manufacturer. In principle steps of VSS [22], the process starts with the cooling of the FDM parts in the refrigeration unit of VSS for 10–15min. The parts after cooling are hanged inside a close chamber (heating unit) wherein the parts are exposed to a standard chemical environment for 10–15sec and then cooled again for 10–15min. The process can be repeated until the required level of surface finish is not achieved.

The present research work is focused to improve the surface finish of FDM parts by using an alternative, cost-effective volatile fluid (acetone). Taguchi L9 OA has been used to study the effect of factors (namely; shape of the geometry (A), density of the parts (B) and chemical exposure time (C)) on surface finish and dimensional accuracy of the selected benchmarks parts.

2. Materials and methods

In the present research work, Stratasys Inc. VSS (specifications given in Table 1) was used for improving the surface finish. VSS process is known for improving the surface finish to about 15 times but the high cost of standard volatile fluid is the only obstacle presented till date. The VSS used in the present research work does not allow the users to alter cooling temperature and heating temperature however an alternative fluid can be used in order to make the process economical. The standard material of VSS is highly volatile which starts to evaporate above 17–20 °C. It has been observed that acetone ($(CH_3)_2CO$) possessed similar volatility. So, in the present research work acetone was selected as the alternative VSS fluid from the available categories of volatile material.

A typical chemical specifications of acetone used in present study is illustrated in Table 2. Initially, three different benchmark geometries including: cube, cylinder and hemi-sphere (all of same volume i.e. 16579.2 mm^3) were selected. Stratasys Inc. uPrint-SE-FDM system (with ABS-P400 material) was used for the prototyping of the benchmark components at three different available densities (low, solid and high) with 0.254 mm layer thickness at 0° build orientation (best in-terms of surface finish). The surface roughness and dimensional accuracy of the fabricated benchmarks was tested before their chemical treatment. Table 3 shows the initial surface roughness and dimensional values of the benchmarks. In chemical treatment, benchmarks were cooled for 10min in the refrigerator unit of VSS prior to their exposure to volatile acetone vapor environment (AVE). After cooling, the benchmarks patterns were hanged inside the heating chamber wherein the

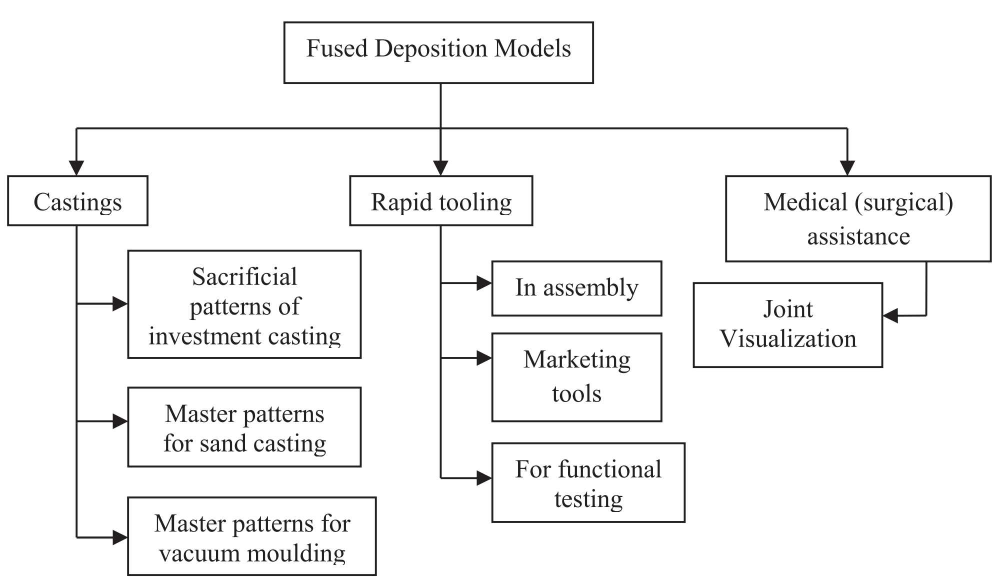

Fig. 1. Applications of FDM parts.

Table 1
Specification of VSS (Stratasys Inc.).

Part/Factor	Specification
Chamber size	330 × 406 × 508 mm
Smoothing fluid	Highly volatile (patented by Stratasys Inc.)
Smoothing fluid cost	370 US$/20lt.
System size/weight	1511.3 × 1092 × 1485.89mm/272.16 kg
Operating environment	• Good ventilation • Maximum room temperature 29.4 °C • humidity <65% non-condensing • Maximum altitude of 3280 m
Power requirements	200-240 VAC, 50/60 Hz, 20 amp
Cooling chamber temperature (refrigeration unit)	0-4 °C
Smoothing chamber temperature	45-50 °C
Fluid capacity	10lt (min.)

Table 2
Specification of acetone[a].

Properties/Chemical/Factor	Specification
Assay (GLC)	99% (min)
Boiling range (95%)	55.5–56.5 °C
Weight/ml at 20 °C	0.790–0.792 gm
Acidity (CH_3COOH)	0.01% (max.)
N.V.M	0.002% (max.)
Water	0.5% (max.)
Solution	Clear & Colorless
Cost	103 US$/20lt.

[a] Resource: Nice Chemicals (P) Ltd., Kerala, India.

vapors of volatile acetone chemical re-flowed the material. Then the benchmarks were again cooled in the refrigerator chamber for 10min in order to allow the fixation of re-flowed material. In the trials runs, the FDM parts were exposed to AVE for 25, 30 and 35sec. From scanning electron microscopic (SEM) analysis, it has been found that the surfaces of FDM parts were deteriorated due to prolonged processing. Fig. 2 shows the SEM micrograph of deteriorated FDM surface (maximum with 35sec). On the basis of the trial runs, the maximum level of AVE was kept as 20sec.

In final experimentation, Taguchi L9 OA has been used to identify the optimum processing conditions of FDM parts in VSS in response of obtaining better surface finish with negligible dimensional variations. Table 4 shows the control log of experimentation. Whereas, Table 5 shows the final results of surface roughness and dimensional features measured after 24 h of chemical processing.

3. Results and discussions

Surface roughness and dimensional accuracy of benchmarks was measured using Mitutoyo-SJ-210 roughness tester (as per ISO-1997 at 0.5 mm/s stylus speed and 0.25 mm cut-off length) and Mitutoyo Vernier caliper (accurate up-to 0.01 mm) respectively. In the present research work, improvement in surface finish and deviations encountered after vapor processing were quantified by subtracting the initial and final values by using the following Eqn. (1):

$$\text{Percentag echange} = \left[(\text{Initial value} - \text{Final value}) / \text{Intial value} \times 100 \right] \quad (1)$$

For dimensional analysis, height of the benchmarks was selected judicially. Minitab-17 statistical software package was used to find out the effect of processing parameters (i.e. A, B and C) on the quality characteristics of the patterns. Table 6 shows the improved value of surface finish of the patterns, dimensional deviation and their respective signal to noise (S/N) responses.

Fig. 3(a) and (b) shows the main effect of S/N ratio on selected process parameters for surface roughness and dimensional deviation respectively. Further ANOVA has been conducted for calculating the percentage contribution of input process parameters in surface roughness and dimensional deviation, shown in Tables 7 and 8 respectively. Parametric response of S/N ratio for surface roughness and dimensional deviation is given in Tables 9 and 10 respectively.

From Table 7, it has been found that out of three input selected parameters only AVE is found to have significant affected on the surface roughness of benchmark. From Table 7, it has been observed that parameter A and B are in-significant for the surface roughness. Further their percentage contribution is also negligible. However, in case of parameter C, it has been found that the surface finish of the benchmarks increases with an increase in the AVE. The major reason behind this trend is due to the fact that with an increase in

Table 3
Results of initial measurements.

S. No.	A	B	Surface roughness (μm), avg.	Dimension (mm), avg.
1	Cube	Low density	8.45	h-25.80
2	Cube	Solid density	9.186	h-25.60
3	Cube	High density	8.835	h-25.89
4	Cylinder	Low density	8.601	ϕ-29.96 and h-23.69
5	Cylinder	Solid density	8.593	ϕ-29.93 and h-23.76
6	Cylinder	High density	8.756	ϕ-29.92 and h-23.82
7	Hemi-sphere	Low density	8.591	ϕ-39.86 and h-20.41
8	Hemi-sphere	Solid density	8.336	ϕ-39.80 and h-20.42
9	Hemi-sphere	High density	8.149	ϕ-39.82 and h-20.41

Note: The parameter ‘A’ represents three geometrical shapes and parameter ‘B’ represents three densities, which is basically a feature available in software of commercial FDM setup. All components were prepared at 0° inclination along X-axis (horizontal orientation).
Where, ‘ϕ’ is diameter and ‘h’ is height.

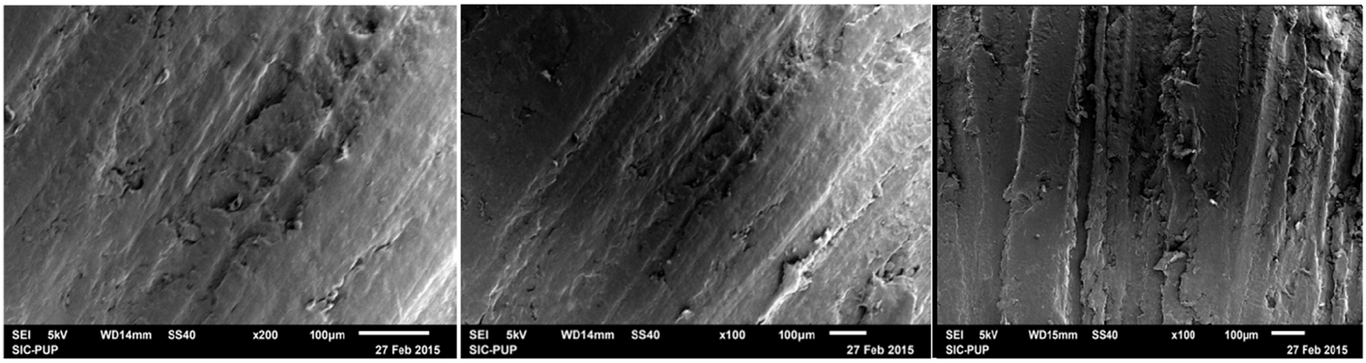

Fig. 2. (a) SEM micrograph of FDM part exposed to 25 (b) 30 and (c) 35sec.

Table 4
Control log of experimentation.

S. No.	A	B	Chemical exposure time (C), sec.
1	Cube	Low density	10
2	Cube	Solid density	15
3	Cube	High density	20
4	Cylinder	Low density	15
5	Cylinder	Solid density	20
6	Cylinder	High density	10
7	Hemi-sphere	Low density	20
8	Hemi-sphere	Solid density	10
9	Hemi-sphere	High density	15

the AVE cycle time sufficient time was available for the re-flow mechanism. The SEM analysis (with transverse view) of the finished FDM benchmark component (as shown in Fig. 4) shows that exposing of FDM parts to AVE in VSS have re-flowed the material and resulted into the formation of a fine layer of on the surface of FDM parts.

It can be seen from Fig. 4 that the thickness of re-flow layer increases with AVE exposure time. With an increase in the AVE time the depth of penetration also increased due to which more number of layers started to reflow hence the thickness of re-flow layer increased (as shown in Fig. 4). However, the prolonged exposure time may have some affect the mechanical properties (like: dimensional accuracy, tensile strength, compressive strength, elongation, hardness, etc.) which are yet to explore.

The optimized settings for surface roughness of vapor smoothened FDM benchmark parts are: A > cylinder, B > high density and C > 20sec. However, in case of dimensional deviation, none of parameter was found to have significant affect (as given in Table 8) on the geometrical features of the benchmark components. The optimized settings for dimensional deviation are: A > hemi-sphere, B > solid density and C > 10sec.

Hence, the optimum condition of input process parameters for

Table 5
Results of final measurements.

S. No.	A	B	C	Surface roughness (μm), avg.	Dimension (mm), avg.
1	Cube	Low density	10	0.39	h-25.75
2	Cube	Solid density	15	0.19	h-25.53
3	Cube	High density	20	0.07	h-25.45
4	Cylinder	Low density	15	0.18	ϕ-29.82 and h-23.63
5	Cylinder	Solid density	20	0.069	ϕ-29.82 and h-23.71
6	Cylinder	High density	10	0.24	ϕ-29.83 and h-23.76
7	Hemi-sphere	Low density	20	0.08	ϕ-39.77 and h-20.30
8	Hemi-sphere	Solid density	10	0.31	ϕ-39.76 and h-20.31
9	Hemi-sphere	High density	15	0.17	ϕ-39.77 and h-20.25

Where, 'ϕ' is diameter and 'h' is height.

Table 6
Improved value of surface roughness, dimensional deviation and their respective S/N response.

S. No.	Improvement in surface roughness (%)	S/N ratio, db	Dimensional deviation (%)	S/N ratio, db
1	95.38	39.58	0.19	14.42
2	97.93	39.81	0.27	11.37
3	99.20	39.93	1.69	−4.55
4	97.90	39.81	0.46	6.74
5	99.19	39.92	0.36	8.87
6	97.25	39.75	0.30	10.45
7	99.06	39.91	0.22	13.15
8	96.28	39.67	0.10	20.00
9	97.91	39.81	0.12	18.41
Overall mean of S/N ratio for surface roughness is 39.8050			Overall mean of S/N ratio for dimensional deviation is 10.98	

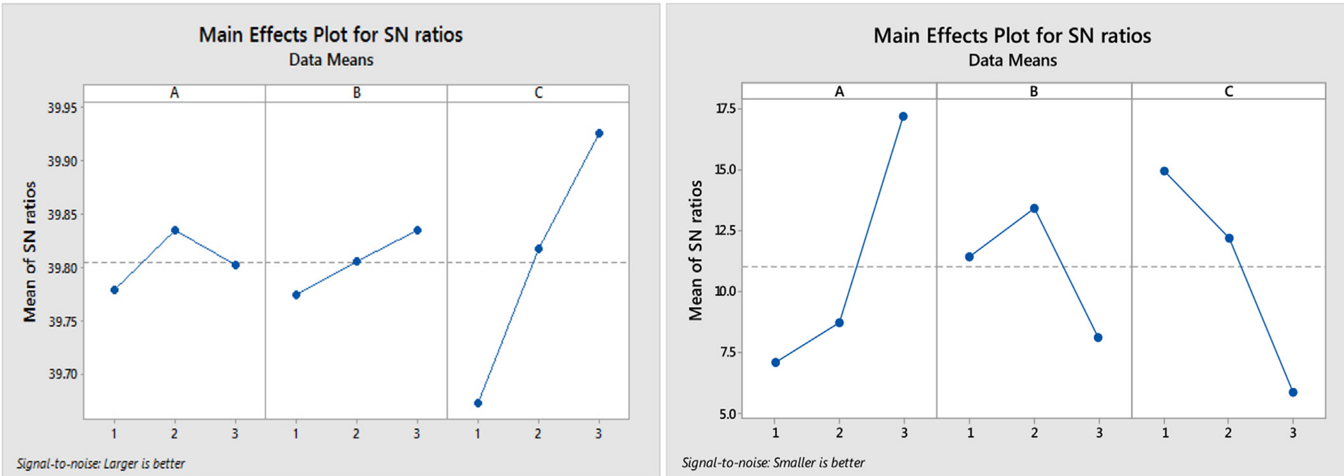

(a) (b)

Fig. 3. (a) Main effect of S/N ratio on input process parameters for surface roughness (b) for dimensional deviation.

Table 7
ANOVA for surface roughness.

Source	Degree of freedom	Sum of square	Variance	F-value	P-value	Percentage contribution (%)	Significance (Yes/No)
A	2	0.004594	0.002297	1.09	0.479	4.13	No
B	2	0.005514	0.002757	1.31	0.433	4.95	No
C	2	0.096863	0.048431	22.98	0.042	87.11	Yes
Error	2	0.004216	0.002108			3.79	
Total	8	0.111186					

Table 8
ANOVA for dimensional deviation.

Source	Degree of freedom	Sum of square	Variance	F-value	P-value	Percentage contribution (%)	Significance (Yes/No)
A	2	177.00	88.50	2.70	0.27	42.39	No
B	2	43.22	21.61	0.66	0.61	10.35	No
C	2	131.64	65.82	2.01	0.34	31.49	No
Error	2	65.60	32.80			15.71	
Total	8	417.46					

Table 9
Response table of S/N ratio for surface roughness.

Level	A	B	C
1	39.78	39.77	39.67
2	39.83[a]	39.81	39.82
3	39.80	39.83[a]	39.93[a]
Delta	0.06	0.06	0.25
Rank	3	2	1

[a] Indicating the optimum response.

Table 10
Response table of S/N ratio for dimensional deviation.

Level	A	B	C
1	7.08	11.44	14.96
2	8.69	13.42[a]	12.178[a]
3	17.189[a]	8..11	5.83
Delta	10.11	5.31	9.14
Rank	1	3	2

[a] Indicating the optimum response.

surface roughness is $A_2B_3C_3$. The theoretical value of 'η' under the optimum conditions, denoted by 'η_{opt}' could be calculated from following Eqn. (2):

$$\eta_{opt} = m + (m_{A2} - m) + (m_{B3} - m) + (m_{C3} - m) = 39.98db \quad (2)$$

Where m is the overall mean of S/N data (refer Table 6), m_{A2} is the mean of S/N data for factor A at level 2 and m_{B3} is the mean of S/N data for factor B at level 3, etc (refer Table 9).

The corresponding value of surface roughness is given by following Eqn. (3):

$$y_{opt}^2 = 1 \Big/ 10^{-\eta_{opt}/10} \quad (3)$$

And, $y_{opt} = 0.010$ m (predicted value).

A confirmatory experiment was performed at the optimized setting which resulted into surface roughness as 0.01 μm. Fig. 5 shows roughness profile along with the SEM micrograph taken for confirmatory experiment prior and after vapor smoothening. In Fig. 5, the stair-case gap between two adjacent layers has been filled upon its chemical exposure due to the re-flow mechanism. This ensured the sensitivity of the ABS-P400 material towards acetone fluid. Presently, the processing parameter of VSS was

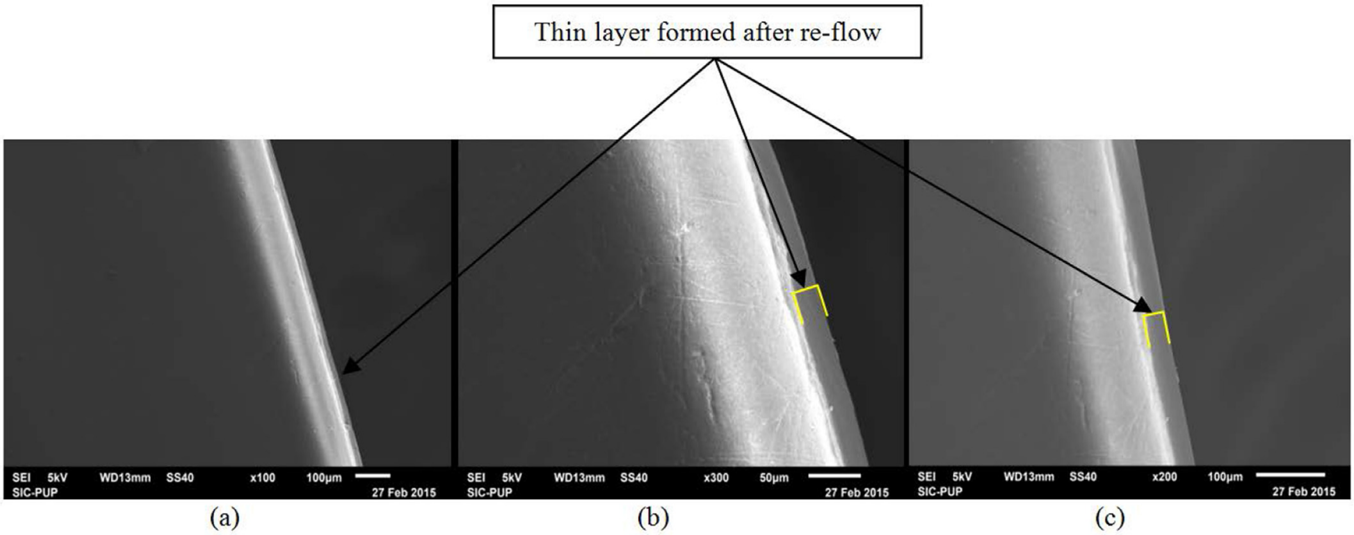

Fig. 4. (a) SEM micrographs of FDM part processed for 10 (b) 15 and (c) 20sec.

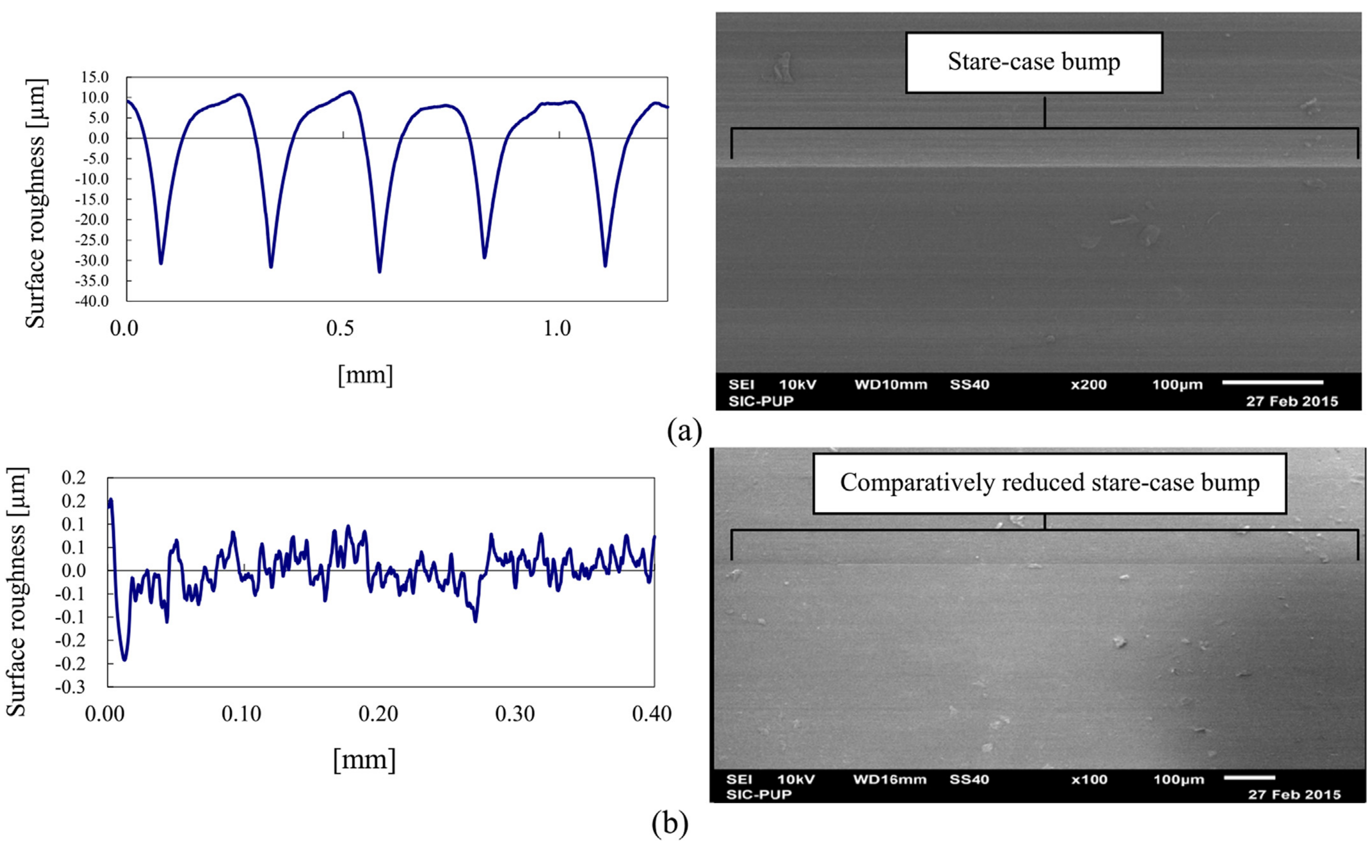

Fig. 5. Roughness profile before vapor processing (a) after vapor processing (b).

selected so that the re-flow of the material is just limited to the surface of the benchmarks.

4. Conclusions

From the present research work following conclusions may be drawn:

In this paper a chemical treatment of FDM patterns has been carried out for improving their surface finish. The results of present study highlighted that VSS and FDM patterns has been successfully coupled and quality characteristics concerned to surface finish has been improved to nano-level without affecting the dimensional features. The experimental study was conducted for finding the optimum processing condition in-terms of shape of geometry, FDM system density and chemical exposure cycle. ANOVA highlighted that only chemical exposure cycle has significantly affected the surface finish of the patterns. Profilometer measurements made incase of confirmatory experimentation showed the decrease in roughness profile of the patterns after their chemical treatment. The SEM micrographs highlighted the re-flow of the ABS material resulted into formation of thin layer on the surface which improved the aesthetic look of the benchmarks. Further, the S/N response highlighted the negligible change in the dimensional features of the patterns exposed to AVE.

Results of the present study explored the benefits of VSS for FDM parts to be used as either sacrificial pattern in investment casting process, and rapid manufacturing of innovative materials and structures [23–36]. Further, the use of an alternative volatile fluid like acetone has effectively reduced the processing cost of VSS. Confirmatory experimentation showed a very good agreement between the predicted and experimental value.

Acknowledgements

The authors are thankful to All India Council for Technical Education (NCP grant) for financial support.

References

[1] Boschetto A, Giordano V, Veniali F. Int J Adv Manuf Technol 2012;61:945–56.
[2] Gebhardt A. Rapid prototyping. Hanser, Munich. 2003.
[3] Hopkinson N, Hague R, Dickens P. Rapid manufacturing an industrial revolution for the digital age. Chichester, West Sussex: John Wiley & Sons; 2005.
[4] Wholers T. Wohlers report 2006: rapid prototyping & manufacturing state of the industry annual worldwide progress report. Wohlers Associates, Inc. Fort Collins, CO; 2006.
[5] Wohlers T. Wohlers report 2012: executive summary. Fort Collins, CO: Wohlers Associates, Inc; 2012.
[6] Boschetto A, Giordano V, Veniali F. Rapid Prototyp J 2013;19(4):240–52.
[7] Chua CK, Leong KF, Lim CS. Rapid prototyping: principles and applications. third ed. Singapore: World Scientific; 2010.
[8] Ingole DS, Kuthe AM, Thakare SB, Talankar AS. Rapid Prototyp J 2009;15(4): 280–90.
[9] Ivanova O, Williams C, Campbell T. Rapid Prototyp J 2013;19(5):353–64.
[10] Lee BH, Abdullah J, Khan ZA. J Material Process Technol 2005;169:54–61.
[11] Huang X, Ye C, Wu S, Guo K, Mo J. Int J Adv Manuf Technol 2009;42:1074–81.
[12] Pandey PM, Reddy NV, Dhande SG. Int J Mach Tools Manuf 2003;43(1):61–71.
[13] Galantucci LM, Lavecchia F, Percoco G. CIRP Annals-Manufacturing Technol 2000;59(1):247–50.
[14] Vasudevarao B, Natarajan DP, Henderson M. Sensitivity of RP surface finish to process parameter variation. Austin, USA. In: Proceedings of solid free form fabrication; 2000. p. 252–8.
[15] Anitha R, Arunachalam S, Radhakrishnan P. J Material Process Technol 2001;118:385–8.
[16] Ahn DK, Kim H, Lee S. J Mater Process Technol 2009;209:664–71.
[17] Campbell RI, Martorelli M, Lee HS. Computer-Aided Des 2002;34:717–25.
[18] Anoop KS, Ohdar RK, Mahapatra SS. Mater Des 2009;30(10):4243–52.
[19] Ippolito R, Iuliano L, Gatto A. CIRP Annals-Manufacturing Technol 1995;44(1): 157–60.
[20] Pennington RC, Hoekstra NL, Newcomer JL. Proceedings of the institution of mechanical engineers, Part E. J Process Mech Eng 2005;219(1):89–92.
[21] Thrimurthulu K, Pandey PM, Reddy NV. Int J Mach Tools Manuf 2004;44(6): 585–94.
[22] Zinniel RL. Vapor smoothing surface finishing system. U.S. Patent No. 8075300 B2. 2011.
[23] Singh R, Singh S, Fraternali F-. Development of in-house composite wire based feed stock filaments of fused deposition modelling for wear-resistant materials and structures. Composites. Part B. Engineering 2016;98:244–9.
[24] Singh R, Kumar R, Feo L, Fraternali F. Friction welding of dissimilar plastic/polymer materials with metal powder reinforcement. Compos Part B, Eng 2016;101:77–86.
[25] Fraternali F, Farina I, Polzone C, Pagliuca E, Feo L. On the use of R-PET strips for the reinforcement of cement mortars Composites. Part B. Engineering 2013;46:207–10.
[26] Farina I, Fabbrocino F, Carpentieri G, Modano M, Amendola A, Goodall R, et al. On the reinforcement of cement mortars through 3D printed polymeric and metallic fibers. Compos Part B, Eng 2016;90:76–85.
[27] Farina I, Fabbrocino F, Colangelo F, Feo L, Fraternali F. Surface roughness effects on the reinforcement of cement mortars through 3D printed metallic fibers. Compos Part B, Eng 2016;99:305–11.
[28] Fabbrocino F, Farina I, Amendola A, Feo L, Fraternali F. Optimal design and additive manufacturing of novel reinforcing elements for composite materials, ECCOMAS Congress 2016 – European Congress on Computational Methods in Applied Sciences and Engineering, 5–10 JUNE 2016 Crete Island, Greece, No. 4544 (16 pages).
[29] Schmidt B, Fraternali F. Universal formulae for the limiting elastic energy of membrane networks. J Mech Phys Solids 2012;60:172–80.
[30] Fraternali F. Free discontinuity finite element models in two-dimensions for in-plane crack problems. Theor Appl Fract Mech 2007;47:274–82. 2007.
[31] Fraternali F, Reddy JN. A penalty model for the analysis of laminated composite shells. Int J Solids Struct 1993;30:3337–55.
[32] Amendola A, Nava EH, Goodall R, Todd I, Skelton RE, Fraternali F. On the additive manufacturing and testing of tensegrity structures. Compos Struct 2015;131:66–71.
[33] Amendola A, Smith CJ, Goodall R, Auricchio F, Feo L, Benzoni G, et al. Experimental response of additively manufactured metallic pentamode materials confined between stiffening plates. Compos Struct 2016;142:254–62.
[34] Amendola A, Fabbrocino F, Feo L, Fraternali F. Dependence of the mechanical properties of pentamode materials on the lattice microstructure, ECCOMAS Congress 2016 – European Congress on Computational Methods in Applied Sciences and Engineering, 5–10 JUNE 2016 Crete Island, Greece, No. 6004 (17 pages).
[35] Amendola A, Carpentieri G, Feo L, Fraternali F. Bending dominated response of layered mechanical metamaterials alternating pentamode lattices and confinement plates. Online first Compos Struct 2016;157:71–7.
[36] Fabbrocino F, Amendola A, Benzoni G, Fraternali F. Seismic application of pentamode lattices. Ingegneria Sismica/International J Earthq Eng 2016;1–2: 62–71. ISSN: 0393-1420.